

CORONAL HEATING VERSUS SOLAR WIND ACCELERATION

Steven R. Cranmer

Harvard-Smithsonian Center for Astrophysics, Cambridge, MA 02138, USA; Email: scranmer@cfa.harvard.edu
 To be published in the proceedings of *SOHO-15: Coronal Heating*, 6–9 Sept. 2004, St. Andrews, Scotland, ESA SP-575

ABSTRACT

Parker's initial insights from 1958 provided a key causal link between the heating of the solar corona and the acceleration of the solar wind. However, we still do not know what fraction of the solar wind's mass, momentum, and energy flux is driven by Parker-type gas pressure gradients, and what fraction is driven by, e.g., wave-particle interactions or turbulence. *SOHO* has been pivotal in bringing these ideas back to the forefront of coronal and solar wind research. This paper reviews our current understanding of coronal heating in the context of the acceleration of the fast and slow solar wind. For the fast solar wind, a recent model of Alfvén wave generation, propagation, and non-WKB reflection is presented and compared with UVCS, SUMER, radio, and *in situ* observations at the last solar minimum. The derived fractions of energy and momentum addition from thermal and non-thermal processes are found to be consistent with various sets of observational data. For the more chaotic slow solar wind, the relative roles of steady streamer-edge flows (as emphasized by UVCS abundance analysis) versus bright blob structures (seen by LASCO) need to be understood before the relation between streamer heating and slow-wind acceleration can be known with certainty. Finally, this presentation summarizes the need for next-generation remote-sensing observations that can supply the tight constraints needed to unambiguously characterize the dominant physics.

Key words: coronal heating; MHD waves; solar corona; solar wind; plasma physics; turbulence; UV spectroscopy.

1. INTRODUCTION

The origin of coronal heating is intimately linked to the existence and physical cause of the acceleration of the solar wind. The early history of both “unsolved problems” reaches back into the 19th century (e.g., Hufbauer 1991; Parker 1999, 2001; Soon and Yaskell 2004). Parker (1958, 1963) combined existing empirical clues concerning an outflow of particles from the Sun with the earlier discovery of a hot corona to postulate his transonic flow solution. (An explicit closed-form solution to the isothermal Parker solar wind equation was derived by Cranmer 2004.) In Parker's original models, gravity was counteracted solely by the large gas pressure gradient of the million-degree corona, and wind speeds up to ~ 1000 km/s were possible with mean coronal temperatures of order 3–4 million K.

Mariner 2 confirmed the existence of a continuous supersonic solar wind just a few years after Parker's initially controversial work, and also showed that the wind exists in two relatively distinct states: slow (300–500 km/s) and fast (600–800 km/s). The succeeding decades saw a more comprehensive *in situ* exploration of the solar wind. Before the late 1970s, though, the slow-speed component of the wind was believed to be the “quiet” background state of the plasma; the high-speed streams were seen as occasional disturbances (see Hundhausen 1972). This view was bolstered by increasing evidence that average coronal temperatures (in open magnetic regions feeding the solar wind) probably did not exceed ~ 2 million K, thus making the slow wind easier to explain with Parker's basic theory. However, we know now that this idea came from the limited perspective of spacecraft that remained in or near the ecliptic plane; it gradually became apparent that the fast wind is indeed the more “ambient” steady state (e.g., Feldman et al. 1976; Axford 1977). The polar passes of *Ulysses* in the 1990s confirmed this revised paradigm (Gosling 1996; Marsden 2001).

In the 1970s and 1980s, it became increasingly evident that even the most sophisticated solar wind models could not produce a *fast wind* without the deposition of heat or momentum in some form into the corona (e.g., Holzer and Leer 1980). It is still unclear what fraction of the fast wind's acceleration comes from the gas pressure gradient (i.e., from coronal heating) and what fraction is directly added to the plasma from some other source (usually believed to be waves). This paper surveys our current understanding of the fast wind with an eye on the relative impact of coronal heating (§ 2) and external momentum deposition (§ 3). A brief review of *SOHO* results concerning slow wind acceleration—highlighting the similarities and differences between the fast and slow wind—is given in § 4. Conclusions and a “wish list” of key measurements for future missions are given in § 5.

2. FAST WIND: CORONAL HEATING

Much of the *SOHO-15* Workshop was devoted to studying the so-called “basal” coronal heating problem; i.e., the physical origin of the heat deposited below a heliocentric distance of about $1.5 R_{\odot}$. At these heights, different combinations of mechanisms (e.g., magnetic reconnection, turbulence, wave dissipation, and plasma instabilities) are probably responsible for the varied appearance of coronal holes, quiet regions, isolated loops, and active regions (Priest et al. 2000; Aschwanden et al. 2001; Cargill and Klimchuk 2004). In the open magnetic flux tubes that feed the fast solar wind, though, additional heating at distances greater than about $2 R_{\odot}$ is

believed to be needed (Leer et al. 1982; Parker 1991). In coronal holes, the plasma at these larger heights is almost completely collisionless. Thus, the ultimate energy dissipation mechanisms at large heights are probably *qualitatively different* from the smallest-scale collision-dominated mechanisms (i.e., resistivity, viscosity, ion-neutral friction) that act near the base.

The necessity for “extended coronal heating” in addition to that at the base comes from three general sets of empirical constraints (see also Cranmer 2002a).

1. As summarized above, pressure-driven models of the high-speed wind cannot be made consistent with the relatively low inferred temperatures in coronal holes (especially electron temperatures T_e less than about 1.5×10^6 K) without some kind of additional energy deposition. Because electron heat conduction is so much stronger than proton heat conduction, it was realized rather early that one cannot produce the observed *in situ* property of $T_p > T_e$ at 1 AU without additional heating (e.g., Hartle and Sturrock 1968).
2. Spacecraft in the interplanetary medium have measured radial gradients in proton and electron temperatures that are substantially shallower than predicted from pure adiabatic expansion, indicating gradual energy addition (e.g., Phillips et al. 1995; Richardson et al. 1995). *Helios* measurements of radial growth of the proton magnetic moment between the orbits of Mercury and the Earth (Schwartz and Marsch 1983; Marsch 1991) point to specific collisionless processes.
3. *SOHO* has provided more direct evidence for extended heating. UVCS (the Ultraviolet Coronagraph Spectrometer) measured extremely high heavy ion temperatures, faster bulk ion outflow compared to protons, and strong anisotropies (with $T_\perp > T_\parallel$) of ion velocity distributions in the extended corona (Kohl et al. 1997, 1998, 1999; Noci et al. 1997; Li et al. 1998; Cranmer et al. 1999b; Giordano et al. 2000). SUMER (Solar Ultraviolet Measurements of Emitted Radiation) has shown that preferential ion heating may begin very near the limb, in regions previously thought to be in collisional equilibrium and thus dominated by more traditional heating mechanisms (e.g., Tu et al. 1998; Peter and Vocks 2003; Moran 2003; L. Dolla, these proceedings).

The list of possible physical processes responsible for extended coronal heating is limited both by the nearly collisionless nature of the plasma and by the observed temperatures ($T_{\text{ion}} \gg T_p > T_e$). Most suggested mechanisms involve the transfer of energy from *propagating fluctuations*—such as waves, shocks, or turbulent eddies—to the particles. This broad consensus has arisen because the ultimate source of energy must be solar in origin, and thus it must somehow be transmitted out to the distances where the heating occurs (see, e.g., Hollweg 1978a; Tu and Marsch 1995). The *SOHO* observations discussed above have given rise to a resurgence

of interest in collisionless wave-particle resonances (typically the ion cyclotron resonance) as potentially important mechanisms for damping wave energy and preferentially energizing positive ions (e.g., McKenzie et al. 1995; Tu and Marsch 1997, 2001; Hollweg 1999a, 2000; Axford et al. 1999; Cranmer et al. 1999a; Li et al. 1999; Cranmer 2000, 2001, 2002a,b; Galinsky and Shevchenko 2000; Hollweg and Isenberg 2002; Vocks and Marsch 2002; Gary et al. 2003; Marsch et al. 2003; Voitenko and Goossens 2003, 2004; Gary and Nishimura 2004; Gary and Borovsky 2004; Markovskii and Hollweg 2004; see also E. Marsch, these proceedings).

There remains some controversy over whether ion cyclotron waves generated only at the coronal base can heat the extended corona, or if a more gradual generation of these waves is needed over a range of heights. If the latter, then there is also uncertainty concerning the origin of such extended wave generation. MHD turbulence has long been proposed as a likely means of transforming fluctuation energy from low frequencies (e.g., periods of a few minutes; believed to be emitted copiously by the Sun) to the high frequencies required by cyclotron resonance theories (e.g., 10^2 to 10^4 Hz). However, both numerical simulations and analytic descriptions of turbulence indicate that the cascade from large to small length scales occurs most efficiently for modes that do not increase in frequency (for a recent survey, see Oughton et al. 2004). In the corona, the expected type of turbulent cascade would tend to most rapidly increase electron T_\parallel , not the ion T_\perp as observed. Cranmer and van Ballegooijen (2003) discussed this issue at length and surveyed possible solutions.

Much of the work cited above can be broadly summarized as “working backwards” from the measured plasma parameters in the extended corona to deduce the properties of the kinetic-scale fluctuations that would provide the required energy. However, in many models (especially those involving turbulence) the ultimate dissipation at small scales has its origin on much larger scales. It is therefore worthwhile to study the energy input at the largest scales as a constraint on how much deposition will eventually be channeled through the smaller scales.

The remainder of this section is thus devoted to presenting an empirically constrained model of low-frequency (10^{-5} to 1 Hz) Alfvén wave heating in a representative open coronal-hole flux tube (Cranmer and van Ballegooijen 2004). This model follows the radial evolution of the power spectrum of non-WKB Alfvén waves (i.e., waves propagating both outwards and inwards along the flux tube) and allows the turbulent energy injection rate (and thus the heating rate) to be derived as a function of height. The Alfvén waves have their origin in the transverse shaking of strong-field (~ 1500 G) thin flux tubes in the photosphere, and in the supergranular network these flux tubes merge with one another in the mid-chromosphere to form the bases of flux-tube “funnels” that expand outwards into the solar wind (e.g., Hassler et al. 1999; Peter 2001; T. Aiouaz, these proceedings).

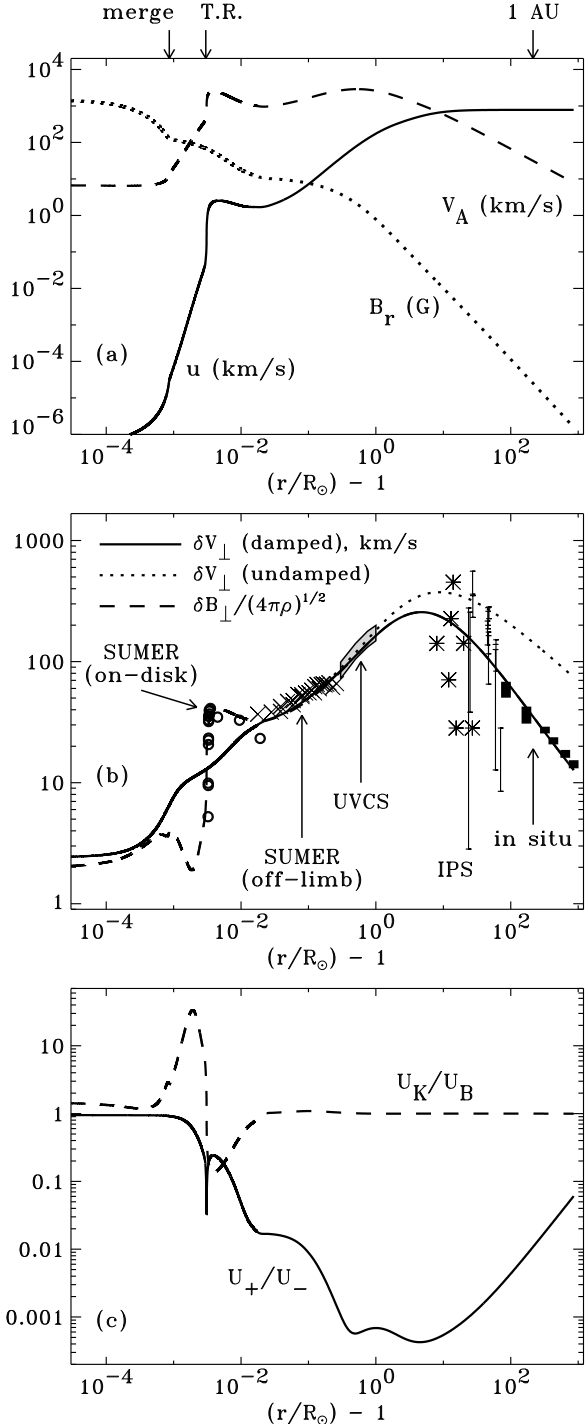


Figure 1. (a) Steady-state plasma conditions along the modeled flux tube: wind speed (solid line), Alfvén speed (dashed line), and magnetic field strength (dotted line). Arrows at the top show the mid-chromospheric “merging height” of thin flux tubes into network funnels, the transition region, and the orbit of the Earth. (b) Frequency-integrated wave amplitudes (see plot for line styles). Observational data points from left to right: circles (Chae et al. 1998), X’s (Banerjee et al. 1998), gray region (Esser et al. 1999), stars (Armstrong and Woo 1981), struts (Canals et al. 2002), filled rectangles (Bavassano et al. 2000). (c) Energy density ratios defined in the plot.

Figure 1 shows a summary of various results from this model. Figure 1a plots the adopted zero-order “background” plasma state (magnetic field strength, wind speed, and Alfvén speed) on which the wave perturbations were placed. The model extends from the photosphere into the outer heliosphere (truncated at 4 AU for convenience). The magnetic field B_r was computed below $1.02 R_\odot$ with a 2.5D magnetostatic model of expanding granular and supergranular flux tubes (see, e.g., Hasan et al. 2003). Above $1.02 R_\odot$, the magnetic field was adopted from the solar-minimum model of Banaszkiewicz et al. (1998). The density was specified empirically from VAL/FAL model C (e.g., Fontenla et al. 1993) at low heights, and white-light polarization brightness measurements at large heights. Mass flux conservation was used to compute the outflow speed, normalized by the solar-minimum *Ulysses* polar mass flux (for more details, see Cranmer and van Ballegooijen 2004).

The bottom boundary condition on the power spectrum of transverse fluctuations came from measurements of G-band bright point motions in the photosphere (e.g., Nissen et al. 2003). The observationally inferred power spectrum was summed from two phases of bright-point motion assumed to be statistically independent: isolated random walks and occasional rapid jumps due to flux-tube merging and fragmenting. Below the mid-chromosphere, where the bright-point flux tubes are isolated and thin, we solved a non-WKB form of the kink-mode wave equations derived by Spruit (1981, 1984). Above the mid-chromosphere, where the flux tubes have merged into a more homogeneous network “funnel,” we solved the wind-modified non-WKB wave transport equations of Heinemann and Olbert (1980). These wave equations were solved for each frequency in a grid spanning periods from 3 seconds to 3 days, and the full radially varying power spectrum was integrated to find the kinetic and magnetic Alfvén wave amplitudes δV_\perp and δB_\perp . Figure 1b shows these amplitudes for both the initial undamped model and another model with turbulent damping (see below). The various observational data points are described in the caption. We note here that the on-disk SUMER nonthermal line widths of Chae et al. (1998) are most probably not transverse Alfvén waves, but their agreement with the *magnetic* fluctuation amplitude in our model may imply some mode coupling between transverse and longitudinal waves. Figure 1c shows the departures from a simple WKB model of purely outward-propagating Alfvén waves. Our model contains linear reflection that produces an inward component of the wave energy density U_+ from the predominantly outward component U_- and does not always exhibit the ideal WKB equipartition between kinetic (U_K) and magnetic (U_B) fluctuations. The total fluctuation energy density is given by $U_K + U_B = U_+ + U_-$.

Note that in Figure 1b the *in situ* measurements fall well below the undamped wave amplitudes. This heliospheric “deficit” of wave power, compared to most prior assumptions about the wave power in the solar atmosphere, is well known (Roberts 1989; Mancuso & Spangler 1999). It seems clear that damping is required in order to agree

with the totality of the measurements, and Cranmer and van Ballegooijen (2004) showed that traditional collisional (i.e., linear viscous) Alfvén wave damping is probably negligible in the fast solar wind. However, if a turbulent cascade has time to develop, the waves can be damped by small-scale kinetic/collisionless processes at a rate governed by the large-scale energy injection rate. The most likely place for this damped wave energy to go is into extended heating.

In a field-free hydrodynamic fluid, turbulent eddies are isotropic and the energy injection rate follows the Kolmogorov (1941) form. This results in a volumetric heating rate ($\text{erg cm}^{-3} \text{ s}^{-1}$)

$$Q_{\text{Kolm}} \approx \frac{\rho \langle \delta V \rangle^3}{\ell} \quad (1)$$

where ρ is the mass density, $\langle \delta V \rangle$ is the r.m.s. fluctuation velocity at the largest scale (called here, possibly imprecisely, the “outer scale”) and ℓ is a representative outer-scale length (i.e., the size of the largest turbulent eddies). Heating rates of this general form were applied quite early in studies of solar wind heating (Coleman 1968) and have been used more-or-less continuously over the past few decades (e.g., Hollweg 1986; Li et al. 1999; Chen and Li 2004).

In a magnetized low-beta plasma, the above Kolmogorov heating rate does not apply because the turbulence is not isotropic. In addition to the well-known MHD anisotropy that allows the cascade to proceed much more efficiently in directions perpendicular to the field than along the field, there is another (possibly more important) departure from isotropy: the outward-propagating Alfvén waves (at outer-scale wavelengths) have a much stronger amplitude than inward-propagating waves. The outer-scale energy injection rate depends critically on the disparity between the outward and inward wave energy densities. In terms of Elsasser’s (1950) variables ($Z_{\pm} \equiv \delta V \pm \delta B / \sqrt{4\pi\rho}$), where Z_- represents outward waves and Z_+ represents inward waves, the energy injection rate for anisotropic MHD turbulence can be written as

$$Q = \alpha \rho \frac{\langle Z_- \rangle^2 \langle Z_+ \rangle + \langle Z_+ \rangle^2 \langle Z_- \rangle}{4\ell_{\perp}} \quad (2)$$

where α is an order-unity calibration factor and ℓ_{\perp} is a purely transverse outer-scale correlation length (see, e.g., Hossain et al. 1995; Matthaeus et al. 1999; Dmitruk et al. 2001, 2002).

In Figure 2 we plot the anisotropic and equivalent Kolmogorov heating rates per unit mass (Q/ρ) for outer-scale lengths that expand with the transverse width of the open flux tube (i.e., $\ell_{\perp} \propto B_r^{-1/2}$). The lengths are normalized so that the damping consistent with the anisotropic heating rate matches the *in situ* amplitudes in Figure 1b. (The resulting normalization yields a value of ℓ_{\perp} at the chromospheric merging height of about 1100 km, which seems appropriate for motions excited between granules of the same spatial scale.) We note that this model is completely consistent only above

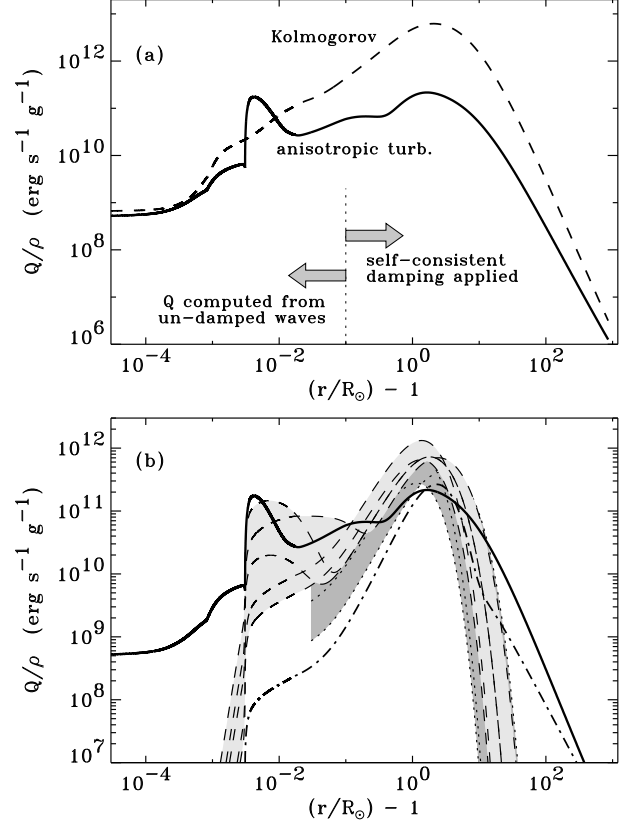


Figure 2. (a) Heating rates per unit mass for the fully anisotropic MHD turbulence model (solid line) and a model that assumes isotropic Kolmogorov turbulence (dashed line). (b) Comparing the same solid line from above with several sets of empirically constrained heating rates: dashed/light-gray (Wang 1994), dotted/dark-gray (Hansteen and Leer 1995), dash-dotted (Allen et al. 1998).

$r = 1.1 R_{\odot}$, where both the damping and the heating were computed together. Below this height, Cranmer and van Ballegooijen (2004) determined that the turbulence would not have time to develop fully, and thus no damping was applied. The heating rates below $1.1 R_{\odot}$ should be considered upper-limit estimates based on the undamped wave amplitudes.

Figure 2a shows the comparison between the anisotropic and Kolmogorov heating rates. The curves are substantially different from one another nearly everywhere, which indicates that the inward/outward imbalance generated by non-WKB reflection is probably a very important ingredient in Alfvén wave heating models of the solar wind. The differences are small in the photosphere and low chromosphere, where strong reflection leads to nearly equal inward and outward wave power. In the extended corona, though, the Kolmogorov heating rate begins to exceed the anisotropic turbulent heating rate by *as much as a factor of 30*. The isotropic Kolmogorov assumption assumes the maximal amount of possible mixing between inward and outward modes, which is incon-

sistent with the relatively weak reflection computed for the corona in our models.

Figure 2b compares the derived anisotropic heating rate with various empirically constrained heating rates—usually specified via sums of exponential functions—from a selection of 1D solar wind models. In these models the parameters of these heating functions were varied freely until sufficiently “realistic” solar wind conditions were produced. A selection of the models presented by Wang (1994) and Hansteen and Leer (1995) are shown, and the SW2 model of Allen et al. (1998) is plotted. The order-of-magnitude agreement, especially in the extended corona at $r \approx 1.5\text{--}4 R_\odot$, indicates that MHD turbulence may be a dominant contributor to the extended heating in the fast wind (see also Dmitruk et al. 2002, for similar comparisons).

3. FAST WIND: DIRECT ACCELERATION

Just as electromagnetic waves carry momentum and exert pressure on matter, acoustic and MHD waves that propagate through an inhomogeneous medium also do work on the fluid via similar radiation stresses. This nondissipative net momentum deposition has been studied for several decades in a solar wind context and is generally called either “wave pressure” or a ponderomotive force (e.g., Bretherton and Garrett 1968; Dewar 1970; Belcher 1971; Alazraki and Couturier 1971; Jacques 1977). Initial computations of the net work done on the bulk fluid have been augmented by calculations of the acceleration imparted to individual ion species (Isenberg & Hollweg 1982; McKenzie 1994; Li et al. 1999; Laming 2004), estimates of the departures from Maxwellian velocity distributions induced by the waves (Goodrich 1978; Hollweg 1978b), and extensions to nonlinearly steepened wave trains (e.g., Koninx 1992).

For non-WKB Alfvén waves propagating along a radially oriented (but potentially superradially expanding) flux tube, Heinemann and Olbert (1980) gave the general expression for the wave pressure acceleration a_{wp} ,

$$\rho a_{wp} = -\frac{\partial U_B}{\partial r} + (U_B - U_K) \frac{\partial}{\partial r}(\ln B_r) \quad (3)$$

where, as above, U_B and U_K are the magnetic and kinetic energy densities of the waves,

$$U_B = \frac{\langle \delta B_\perp \rangle^2}{8\pi} , \quad U_K = \frac{\rho \langle \delta V_\perp \rangle^2}{2} . \quad (4)$$

In the ideal WKB limit (i.e., for purely outward-propagating Alfvén waves), $U_B = U_K$ and only the first term on the right-hand side is present. The above expression also assumes an isotropic pressure (i.e., $T_{\parallel} = T_{\perp}$ for the electrons and protons), but for a low-beta plasma, modest departures from gas-pressure isotropy do not substantially alter the wave pressure. Cranmer and van Ballegooijen (2004) provide plots of a_{wp} versus height for the coronal hole flux tube model discussed in § 2. We summarize those results briefly by mentioning that the weak

degree of reflection in the extended corona (leading to $U_B \approx U_K$ above about $1.05 R_\odot$) validates the use of the simplified WKB form of the wave-pressure acceleration in most solar wind models.

Rather than simply present plots of $a_{wp}(r)$, here we examine the impact of the “known” wave properties on the acceleration region of the solar wind. There are two semi-empirical ways of using the above-described values for $\langle \delta V_\perp \rangle$ and a_{wp} to put constraints on the temperature of the extended corona. Figure 3 shows coronal temperatures derived from the following two methods:

1. UVCS measurements of the widths of the H I Ly α resonance line are useful for their sampling of the motions of hydrogen atoms along the line of sight. For the first few solar radii above the surface, efficient charge exchange processes keep the proton and neutral hydrogen temperatures coupled to one another. For off-limb observations of coronal holes, the line of sight samples mainly directions perpendicular to the nearly radial field lines, and the $1/e$ line width $V_{1/e}$ arises from two primary types of motion:

$$V_{1/e}^2 = \frac{2k_B T_{p\perp}}{m_p} + \langle \delta V_\perp \rangle^2 \quad (5)$$

where k_B is Boltzmann’s constant and m_p is the mass of a proton. The two terms on the right-side represent random “thermal” motions and unresolved transverse wave motions. Using observed values of $V_{1/e}$ and the modeled values of δV_\perp , we can solve the above equation for $T_{p\perp}$. Note that the Cranmer et al. (1999b) data points in Figure 3a were derived from $V_{1/e}$ values that have subtracted out the projected component of the outflow speed along the line of sight; the other values are straightforward line widths.

2. If the steady-state density and outflow speed are known in conjunction with the wave-pressure acceleration, the solar wind momentum conservation equation can be solved empirically for the gas pressure term:

$$\frac{\nabla P}{\rho} = a_{wp} - \frac{GM_\odot}{r^2} - u \frac{du}{dr} \quad (6)$$

(see also Sittler and Guhathakurta 1999, 2002, for similar work). To obtain the pressure P as a function of radius, we integrated ∇P inwards from 1 AU assuming a wide range of possible temperatures at the outer boundary. The resulting coronal $P(r)$ was quite insensitive to the boundary conditions, however, because the gas pressure is so much larger in the corona than at 1 AU. An averaged proton-electron temperature T_{avg} was derived assuming a fully ionized hydrogen-helium plasma:

$$P = n_p k_B T_{\text{avg}} \left[2 + \frac{n_\alpha}{n_p} \left(2 + \frac{T_\alpha}{T_p} \right) \right] \quad (7)$$

where we assumed $n_\alpha/n_p = 0.05$ and we used two extreme values for the alpha-to-proton temperature ratio: 1 and 4.

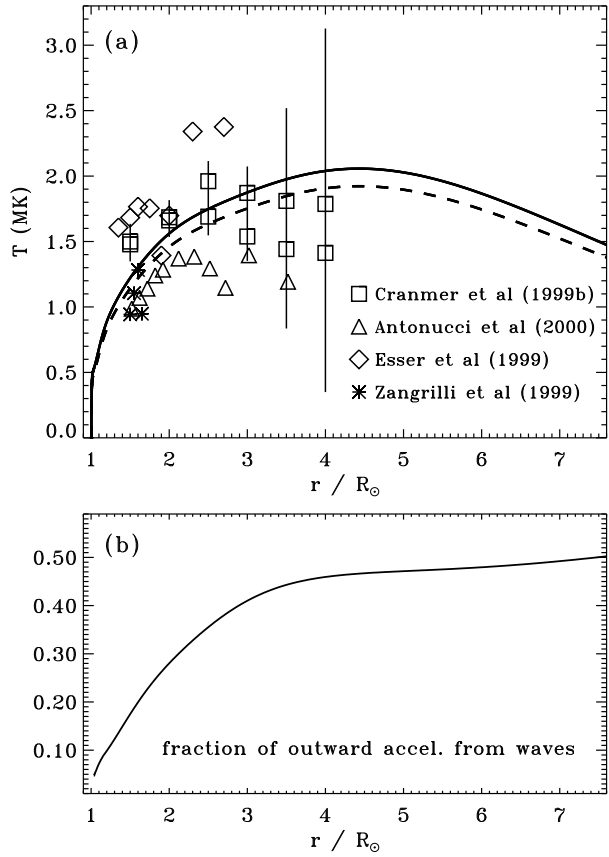


Figure 3. (a) Derived coronal temperatures from UVCS H I Ly α line widths (symbols), and from empirical momentum conservation. For the latter, the two limiting values for the alpha-to-proton temperature ratio T_α/T_p are 1 (solid line), and 4 (dashed line). (b) Fraction of total fast-wind acceleration from wave pressure, i.e., $\rho a_{wp}/(\rho a_{wp} + |\nabla P|)$.

Figure 3a displays the results of both kinds of semi-empirical temperature determination discussed above. The UVCS H I Ly α line width observations (all in solar-minimum polar coronal holes) exhibit a moderate spread that probably can be attributed to different line-of-sight contributions from polar plumes and low count-rate Poisson statistics (as can be seen from the 1σ error bars plotted for the data points of Cranmer et al. 1999b). The overall agreement between both methods of determining the temperature is an adequate consistency check, but note that the UVCS-derived values are specifically proton temperatures, while the momentum-conservation values are essentially $(T_p + T_e)/2$. There is evidence from SUMER and CDS observations below $r \approx 1.5 R_\odot$ that T_e is substantially less than 1 MK, and if this trend continues above $1.5 R_\odot$, it would imply that the momentum-conservation values of T_p must be *larger* than plotted. Thus, the rough agreement between the two methods in Figure 3a may imply that $T_p \approx T_e$ remains the case several solar radii out into the extended corona, in contrast with earlier conclusions that $T_p > T_e$.

Figure 3b shows the fraction of the total outward acceleration (gas pressure + wave pressure) that comes from wave pressure. This plot quantitatively answers the question that was implicitly posed in the title of this paper; i.e., how do coronal heating and direct acceleration “compete” in the fast solar wind? The gas pressure term is decidedly stronger in the first several solar radii (i.e., the primary fast-wind acceleration region), but wave pressure soon reaches a point where it provides roughly half of the acceleration.

All of the above discussion of wave-pressure acceleration was focused solely on Alfvén waves, but it is not yet clear that these are the only MHD wave modes to exist in the extended corona and solar wind. There is some evidence for both fast-mode and slow-mode magnetosonic waves in the corona, but they have been observed mainly in relatively confined regions such as loops and plumes (Ofman et al. 1999; Nakariakov et al. 2004). Fast and slow modes are believed to be more strongly attenuated by collisional damping processes than Alfvén waves before they reach the corona (e.g., Osterbrock 1961; Whang 1997). However, fast-mode waves that propagate *parallel* to the magnetic field behave essentially the same as Alfvén waves (putting aside their kinetic-scale polarization and their preferred cascade directions in k -space), so they may exist at some low level in the corona.

It is worthwhile, at least in a preliminary sense, to compare the wave-pressure accelerations expected from Alfvén waves and from fast-mode waves. For outward-propagating fast-mode waves with an isotropic distribution of wavevectors, Jacques (1977) derived the especially simple expression

$$\rho a_{wp} = \frac{1}{3} \frac{\partial U_B}{\partial r} + \frac{4U_B}{r} \quad (8)$$

in the limit of zero plasma beta and $U_K = U_B$ (note also the opposite sign of the derivative term compared to eq. [3]). The case of an isotropic distribution of wavevectors is likely to be the case for fast-mode waves undergoing a turbulent cascade (e.g., Cho and Lazarian 2003). If we assume that Alfvén and fast-mode waves have identical amplitudes at $r = 2 R_\odot$, and that they both follow their own linear wave-action conservation equations at heights above and below $2 R_\odot$, we can compare their respective values of a_{wp} as a function of height. Figure 4 shows this comparison, and above $r \approx 3 R_\odot$ the fast-mode acceleration is stronger than that of Alfvén waves. This is only an approximate and suggestive result, but it seems to imply that a renewed study of fast-mode waves in the solar wind is warranted (see also Habbal and Leer 1982; Wentzel 1989; Kaghshvili and Esser 2000).

4. SLOW WIND: SIMILARITIES AND DIFFERENCES

The slow-speed component of the solar wind is believed to originate mainly from the bright helmet streamers seen in coronagraph images. However, since these structures are thought to be mainly closed magnetic loops

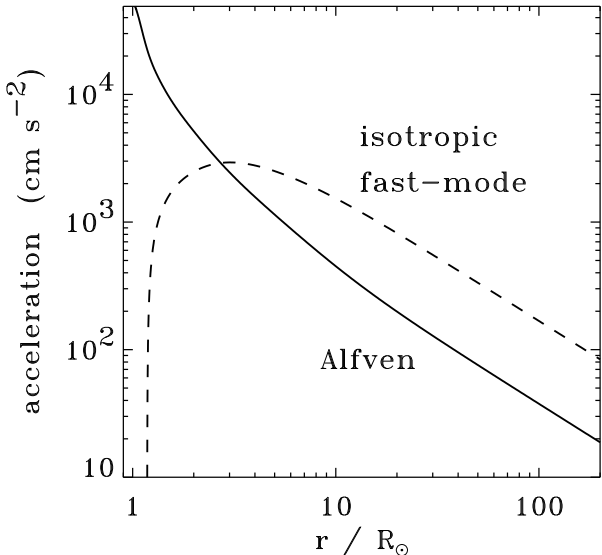


Figure 4. Comparison of ideal WKB wave-pressure acceleration for Alfvén waves (solid line) and an isotropic distribution of $\beta = 0$ fast-mode waves (dashed line). Wave amplitudes were set equal to one another at $r = 2 R_\odot$.

or arcades, it is uncertain how the plasma expands into a roughly time-steady flow. Does the slow wind flow mainly along the open-field edges of these closed regions, or do the closed fields occasionally open up and release plasma into the heliosphere? *SOHO* has provided evidence that both processes occur, but an exact census or mass budget of slow-wind source regions has not yet been constructed. (This is a necessary prerequisite for studying slow-wind “heating versus acceleration.”)

UVCS has shown, at least for the large quiescent equatorial band at solar minimum, that streamers appear differently in the emission of H I Ly α and O VI 1032 Å. The Ly α intensity pattern is similar to that seen in LASCO visible-light images; i.e., the streamer is brightest along its central axis. In O VI, though, there is a darkening in the core whose only interpretation can be a substantial abundance depletion. The solar-minimum equatorial streamers showed an oxygen abundance of 0.3 the photospheric value along the streamer edges, or “legs,” and between 0.01 and 0.1 times the photospheric value in the core (Raymond et al. 1997; Vásquez and Raymond 2004). Low FIP (first ionization potential) elements such as Si and Fe were enhanced by a relative factor of 3 in both cases (Raymond 1999; see also Uzzo et al. 2004). Abundances observed in the legs are consistent with abundances measured in the slow wind *in situ*. This is a strong indication that the majority of the slow wind originates along the open-field edges of streamers. The extremely low abundances in the streamer core, on the other hand, are evidence for gravitational settling of the heavy elements in long-lived closed regions, a result that was confirmed by SUMER (Feldman et al. 1998, 1999).

UVCS measurements have also been used to derive the wind outflow speeds in streamers. Strachan et al. (2002) found zero flow speed at various locations inside in the closed-field core region of an equatorial streamer. Outflow speeds consistent with the slow solar wind were only found along the higher-latitude edges and above the probable location of the magnetic “cusp” between about 3.6 and $4.1 R_\odot$. Frazin et al. (2003) used UVCS to determine that O $^{5+}$ ions in the legs of a similar streamer have significantly higher kinetic temperatures than hydrogen and exhibit anisotropic velocity distributions with $T_\perp > T_\parallel$, much like coronal holes (see also Parenti et al. 2000; L. Strachan, these proceedings). However, the oxygen ions in the closed-field core exhibit neither this preferential heating nor the temperature anisotropy. The analysis of UVCS data has thus led to evidence that the fast and slow wind share at least some of the same physical processes.

Evidence for another kind of slow wind in streamers came from visible-light coronagraph movies. The increased photon sensitivity of LASCO over earlier instruments revealed an almost continual release of low-contrast density inhomogeneities, or “blobs,” from the cusps of streamers (Sheeley et al. 1997; see also Tappin et al. 1999). These features are seen to accelerate to speeds of order 300–400 km/s by the time they reach $\sim 30 R_\odot$. Wang et al. (2000) reviewed three proposed scenarios for the production of these blobs: (1) “streamer evaporation” as the loop-tops are heated to the point where magnetic tension is overcome by high gas pressure; (2) plasmoid formation as the distended streamer cusp pinches off the gas above an X-type neutral point; and (3) reconnection between one leg of the streamer and an adjacent open field line, transferring some of the trapped plasma from the former to the latter and allowing it to escape. Wang et al. (2000) concluded that all three mechanisms might be acting simultaneously, but the third one seems to be dominant. Because of their low contrast, though (i.e., only about 10% brighter than the rest of the streamer), the blobs themselves cannot comprise a large fraction of the mass flux of the slow solar wind. This is in general agreement with the above abundance results from UVCS.

Despite these new observational clues, the overall energy budget in coronal streamers is still not well understood, nor is their temporal MHD stability. Recent models run the gamut from simple, but insightful, analytic studies (Suess and Nerney 2002) to time-dependent multidimensional simulations (e.g., Wiegemann et al. 2000; Lionello et al. 2001; Ofman 2004). Notably, a two-fluid study by Endeve et al. (2004) showed that the stability of streamers may be closely related to the kinetic partitioning of heat to protons versus electrons. When the bulk of the heating goes to the protons, the modeled streamers become unstable to the ejection of massive plasmoids; when the electrons are heated more strongly, the streamers are stable. It is possible that the observed (small) mass fraction of LASCO blobs can give us an observational “calibration” of the relative amounts of heat deposited in the proton and electron populations.

5. CONCLUSIONS AND FUTURE MISSIONS

Our understanding of the dominant physics of solar wind acceleration has progressed rapidly in the *SOHO* era. Unfortunately, the multi-scale *complexity* of the plasma in the extended corona has also been progressively revealed during this same time period. The solar physics community has benefited from increased interaction with the space physics community, the latter having decades more experience grappling with kinetic-scale plasma physics and MHD turbulence. It has been 5 years since Hollweg (1999b) asserted that the “Holy Grail” for theoreticians is the self-consistent modeling of both the full wavenumber spectrum of MHD fluctuations and the spatial dependence of proton, electron, and ion velocity distributions. Much of the recent work cited in this paper, both observational and theoretical, is helping the community get closer to this goal.

The remainder of this section highlights several areas where future space missions (and future ground-based observatories such as ATST) can provide key constraints that refine and test theoretical explanations for solar wind acceleration.

The plasma parameters of both the major species (protons, electrons, and He^{2+}) and minor ions are not yet known in the wind’s acceleration region with sufficient accuracy. Figure 3a highlights the level of our uncertainty about T_p and T_e in coronal holes. Progress in identifying some of the most basic aspects of extended heating can be made only by constraining these basic parameters more tightly. In addition, only by better “filling out” our knowledge of minor ion properties (as a function of ion charge and mass) can we hope to uniquely identify the ultimate kinetic damping mechanisms of waves and/or turbulence (see Cranmer 2001, 2002b). *Spectroscopy is key*—especially in combination with coronagraph occultation—in order to measure line profiles out into the wind’s acceleration region.

The full power spectrum of fluctuations (as a function of distance, wavenumber k_{\parallel} and k_{\perp} , and solar wind type) is a strong driver of solar wind physics, but we still have only indirect constraints on its properties in the corona. The assimilation of multiple data sources, including radio sounding, is crucial (e.g., Spangler 2002, 2003). All previous *in situ* missions that measured wave power spectra in the solar wind have been “contaminated” by the solar rotation, which sweeps new, uncorrelated flux tubes past the spacecraft on time scales of tens of minutes. Cranmer and van Ballegooijen (2004) predicted that much of the measured power with periods longer than about 30 minutes may be due to this effect, and that a spacecraft that could sample the fluctuations in a single flux tube would see intrinsically higher-frequency “fossil” fluctuations from the Sun. Solar *co-rotation* of *in situ* missions (such as Solar Orbiter) may be key, even if the co-rotation is not exact or long-lived.

The origin of waves in jostled photospheric flux-tube motions needs to be pinned down to a much better degree

than at present, in order to put firmer empirical constraints on the “lower boundary condition” of mechanical energy input into the corona. Synergy between 3D convection simulations and high-resolution observations is becoming more common (e.g., Sánchez Almeida et al. 2003). Although space missions may one day boast collecting areas rivaling those of ground-based telescopes, in the near future it is the latter that will push the envelope to provide the necessary constraints. Existing sub-arcsecond spatial resolution needs to be matched by sub-second time resolution, so that the kinetic energy power spectra of small-scale flux tubes (e.g., G-band bright point motions) can be measured more accurately.

ACKNOWLEDGMENTS

This work is supported by the National Aeronautics and Space Administration (NASA) under grants NAG5-11913, NAG5-10996, NNG04GE77G, and NNG04G-E84G to the Smithsonian Astrophysical Observatory, by Agenzia Spaziale Italiana, and by the Swiss contribution to ESA’s PRODEX program.

REFERENCES

- Alazraki, G., Couturier, P., 1971, A&A, 13, 380
- Allen, L. A., Habbal, S. R., Hu, Y. Q., 1998, JGR, 103, 6551
- Antonucci, E., Dodero, M. A., Giordano, S., 2000, Solar Phys., 197, 115
- Armstrong, J. W., Woo, R., 1981, A&A, 103, 415
- Aschwanden, M. J., Poland, A. I., Rabin, D. M., 2001, Ann. Rev. Astron. Astrophys., 39, 175
- Axford, W. I., 1977, in *Study of Travelling Interplanetary Phenomena*, ed. M. A. Shea, D. F. Smart, S. T. Wu (Reidel), 145
- Axford, W. I., McKenzie, J. F., Sukhorukova, G. V., Banaszkiewicz, M., Czechowski, A., Ratkiewicz, R., 1999, Space Sci. Rev., 87, 25
- Banaszkiewicz, M., Axford, W. I., McKenzie, J. F., 1998, A&A, 337, 940
- Banerjee, D., Teriaca, L., Doyle, J. G., Wilhelm, K., 1998, A&A, 339, 208
- Bavassano, B., Pietropaolo, E., Bruno, R., 2000, JGR, 105, 15959
- Belcher, J. W., 1971, ApJ, 168, 509
- Bretherton, F. P., Garrett, C. J. R., 1968, Proc. Roy. Soc. A, 302, 529
- Canals, A., Breen, A. R., Ofman, L., Moran, P. J., Falle, R. A., 2002, Ann. Geophys., 20, 1265
- Cargill, P. J., Klimchuk, J. A., 2004, ApJ, 605, 911
- Chae, J., Schühle, U., Lemaire, P., 1998, ApJ, 505, 957
- Chen, Y., Li, X., 2004, ApJ, 609, L41
- Cho, J., Lazarian, A., 2003, MNRAS, 345, 325
- Coleman, P. J., Jr., 1968, ApJ, 153, 371

- Cranmer, S. R., 2000, *ApJ*, 532, 1197
- Cranmer, S. R., 2001, *JGR*, 106, 24937
- Cranmer, S. R., 2002a, *Space Sci. Rev.*, 101, 229
- Cranmer, S. R., 2002b, in *SOHO-11: From Solar Minimum to Solar Maximum*, ESA SP-508, 361 (arXiv astro-ph/0209301)
- Cranmer, S. R., 2004, *American J. Phys.*, 72, 1397 (arXiv astro-ph/0406176)
- Cranmer, S. R., Field, G. B., Kohl, J. L., 1999a, *ApJ*, 518, 937
- Cranmer, S. R., Kohl, J. L., Noci, G., et al., 1999b, *ApJ*, 511, 481
- Cranmer, S. R., van Ballegooijen, A. A., 2003, *ApJ*, 594, 573
- Cranmer, S. R., van Ballegooijen, A. A., 2004, *ApJ Suppl.*, submitted
- Dewar, R. L., 1970, *Phys. Fluids*, 13, 2710
- Dmitruk, P., Matthaeus, W. H., Milano, L. J., Oughton, S., Zank, G. P., Mullan, D. J., 2002, *ApJ*, 575, 571
- Dmitruk, P., Milano, L. J., Matthaeus, W. H., 2001, *ApJ*, 548, 482
- Elsasser, W. M., 1950, *Phys. Rev.*, 79, 183
- Endeve, E., Holzer, T. E., Leer, E., 2004, *ApJ*, 603, 307
- Esser, R., Fineschi, S., Dobrzycka, D., Habbal, S. R., Edgar, R. J., Raymond, J. C., Kohl, J. L., Guhathakurta, M., 1999, *ApJ*, 510, L63
- Feldman, U., Doschek, G. A., Schühle, U., Wilhelm, K., 1999, *ApJ*, 518, 500
- Feldman, U., Schühle, U., Widing, K. G., Laming, J. M., 1998, *ApJ*, 505, 999
- Feldman, W. C., Asbridge, J. R., Bame, S. J., Gosling, J. T., 1976, *JGR*, 81, 5054
- Feldman, W. C., Marsch, E., 1997, in *Cosmic Winds and the Heliosphere*, ed. J. R. Jokipii, C. P. Sonett, M. S. Giampapa (Univ. Arizona Press), 617
- Fontenla, J. M., Avrett, E. H., Loeser, R., 1993, *ApJ*, 406, 319
- Frazin, R. A., Cranmer, S. R., Kohl, J. L., 2003, *ApJ*, 597, 1145
- Galinsky, V. L., Shevchenko, V. I., 2000, *Phys. Rev. Lett.*, 85, 90
- Gary, S. P., Borovsky, J. E., 2004, *JGR*, 109 (A6), A06105, 10.1029/2004JA010399
- Gary, S. P., Nishimura, K., 2004, *JGR*, 109 (A2), A02109, 10.1029/2003JA010239
- Gary, S. P., Yin, L., Winske, D., Ofman, L., Goldstein, B. E., Neugebauer, M., 2003, *JGR*, 108 (A2), 1068, 10.1029/2002JA009654
- Giordano, S., Antonucci, E., Noci, G., Romoli, M., Kohl, J. L., 2000, *ApJ*, 531, L79
- Goodrich, C. C., 1978, Ph.D. Dissertation, Massachusetts Institute of Technology
- Gosling, J. T., 1996, *Ann. Rev. Astron. Astrophys.*, 34, 35
- Habbal, S. R., Leer, E., 1982, *ApJ*, 253, 318
- Hansteen, V. H., Leer, E., 1995, *JGR*, 100, 21577
- Hansteen, V. H., Leer, E., Holzer, T. E., 1997, *ApJ*, 482, 498
- Hartle, R. E., Sturrock, P. A., 1968, *ApJ*, 151, 1155
- Hasan, S. S., Kalkofen, W., van Ballegooijen, A. A., Ulmschneider, P., 2003, *ApJ*, 585, 1138
- Hassler, D. M., Dammasch, I. E., Lemaire, P., Brekke, P., Curdt, W., Mason, H. E., Vial, J.-C., Wilhelm, K., 1999, *Science*, 283, 810
- Heinemann, M., Olbert, S., 1980, *JGR*, 85, 1311
- Hollweg, J. V., 1978a, *Rev. Geophys. Space Phys.*, 16, 689
- Hollweg, J. V., 1978b, *JGR*, 83, 563
- Hollweg, J. V., 1986, *JGR*, 91, 4111
- Hollweg, J. V., 1999a, *JGR*, 104, 505
- Hollweg, J. V., 1999b, *JGR*, 104, 24781
- Hollweg, J. V., 2000, *JGR*, 105, 15699
- Hollweg, J. V., Isenberg, P. A., 2002, *JGR*, 107 (A7), 1147, 10.1029/2001JA000270
- Holzer, T. E., Leer, E., 1980, *JGR*, 85, 4665
- Hossain, M., Gray, P. C., Pontius, D. H., Jr., Matthaeus, W. H., Oughton, S., 1995, *Phys. Fluids*, 7, 2886
- Hufbauer, K., 1991, *Exploring the Sun: Solar Science since Galileo* (Johns Hopkins Univ. Press)
- Hundhausen, A. J., 1972, *Coronal Expansion and Solar Wind* (Springer-Verlag)
- Isenberg, P. A., Hollweg, J. V., 1982, *JGR*, 87, 5023
- Jacques, S. A., 1977, *ApJ*, 215, 942
- Kaghashvili, E. K., Esser, R., 2000, *ApJ*, 539, 463
- Kohl, J. L., Esser, R., Cranmer, S. R., et al., 1999, *ApJ*, 510, L59
- Kohl, J. L., Noci, G., Antonucci, E., et al., 1997, *Solar Phys.*, 175, 613
- Kohl, J. L., Noci, G., Antonucci, E., et al., 1998, *ApJ*, 501, L127
- Kolmogorov, A. N., 1941, *Dokl. Akad. Nauk SSSR*, 30, 301
- Koninx, J. P. M., 1992, Ph.D. Dissertation, Rijksuniversiteit Utrecht
- Laming, J. M., 2004, *ApJ*, in press (arXiv astro-ph/0405230)
- Leer, E., Holzer, T. E., 1980, *JGR*, 85, 4631
- Leer, E., Holzer, T. E., Flå, T., 1982, *Space Sci. Rev.*, 33, 161
- Li, X., Habbal, S. R., Hollweg, J. V., Esser, R., 1999, *JGR*, 104, 2521
- Li, X., Habbal, S. R., Kohl, J. L., Noci, G., 1998, *ApJ*, 501, L133

- Lionello, R., Linker, J. A., Mikić, Z., 2001, *ApJ*, 546, 542
- Mancuso, S., Spangler, S. R., 1999, *ApJ*, 525, 195
- Markovskii, S. A., Hollweg, J. V., 2004, *ApJ*, 609, 1112
- Marsch, E., 1991, in *Physics of the Inner Heliosphere*, vol. 2, ed. R. Schwenn, E. Marsch (Springer-Verlag), 45
- Marsch, E., Axford, W. I., McKenzie, J. F., 2003, in *Dynamic Sun*, ed. B. N. Dwivedi (Cambridge Univ. Press), 374
- Marsden, R. G., 2001, *Astrophys. Space Sci.*, 277, 337
- Matthaeus, W. H., Zank, G. P., Oughton, S., Mullan, D. J., Dmitruk, P., 1999, *ApJ*, 523, L93
- McKenzie, J. F., 1994, *JGR*, 99, 4193
- McKenzie, J. F., Banaszkiewicz, M., Axford, W. I., 1995, *A&A*, 303, L45
- Moran, T. G., 2003, *ApJ*, 598, 657
- Nakariakov, V. M., Arber, T. D., Ault, C. E., Katsiyannis, A. C., Williams, D. R., Keenan, F. P., 2004, *MNRAS*, 349, 705
- Nisenson, P., van Ballegooijen, A. A., de Wijn, A. G., Süitterlin, P., 2003, *ApJ*, 587, 458
- Noci, G., et al., 1997, *Adv. Space Res.*, 20 (12), 2219
- Ofman, L., 2004, *Adv. Space Res.*, 33 (5), 681
- Ofman, L., Nakariakov, V. M., DeForest, C. E., 1999, *ApJ*, 514, 441
- Osterbrock, D. E., 1961, *ApJ*, 134, 347
- Oughton, S., Dmitruk, P., Matthaeus, W. H., 2004, *Phys. Plasmas*, 11, 2214
- Parenti, S., Bromage, B. J. I., Poletto, G., Noci, G., Raymond, J. C., Bromage, G. E., 2000, *A&A*, 363, 800
- Parker, E. N., 1958, *ApJ*, 128, 664
- Parker, E. N., 1963, *Interplanetary Dynamical Processes* (Interscience)
- Parker, E. N., 1991, *ApJ*, 372, 719
- Parker, E. N., 1999, in *Solar Wind Nine*, ed. S. Habbal, R. Esser, J. Hollweg, and P. Isenberg, AIP Conf. Proc. 471, 3
- Parker, E. N., 2001, *JGR*, 106, 15797
- Peter, H., 2001, *A&A*, 374, 1108
- Peter, H., Vocks, C., 2003, *A&A*, 411, L481
- Phillips, J. L., Feldman, W. C., Gosling, J. T., Scime, E. E., 1995, *Adv. Space Res.*, 16 (9), 95
- Priest, E. R., Foley, C. R., Heyvaerts, J., Arber, T. D., Mackay, D., Culhane, J. L., Acton, L. W., 2000, *ApJ*, 539, 1002
- Raymond, J. C., 1999, *Space Sci. Rev.*, 87, 55
- Raymond, J. C., Kohl, J. L., Noci, G., et al., 1997, *Solar Phys.*, 175, 645
- Richardson, J. D., Paularena, K. I., Lazarus, A. J., Belcher, J. W., 1995, *GRL*, 22, 325
- Roberts, D. A., 1989, *JGR*, 94, 6899
- Sánchez Almeida, J., Emonet, T., Cattaneo, F., 2003, *ApJ*, 585, 536
- Schwartz, S. J., Marsch, E., 1983, *JGR*, 88, 9919
- Sheeley, N. R., Jr., Wang, Y.-M., Hawley, S. H., et al., 1997, *ApJ*, 484, 472
- Sittler, E. C., Jr., Guhathakurta, M., 1999, *ApJ*, 523, 812
- Sittler, E. C., Jr., Guhathakurta, M., 2002, *ApJ*, 564, 1062
- Soon, W. W.-H., Yaskell, S. H., 2004, *The Maunder Minimum and the Variable Sun-Earth Connection* (World Scientific)
- Spangler, S. R., 2002, *ApJ*, 576, 997
- Spangler, S. R., 2003, *Nonlin. Proc. Geophys.*, 10, 179
- Spruit, H. C., 1981, *A&A*, 98, 155
- Spruit, H. C., 1984, in *Small-scale Dynamical Processes in Quiet Stellar Atmospheres*, ed. S. L. Keil (NSO), 249
- Strachan, L., Panasyuk, A. V., Dobrzycka, D., Kohl, J. L., Noci, G., Gibson, S. E., Biesecker, D. A., 2000, *JGR*, 105, 2345
- Strachan, L., Suleiman, R., Panasyuk, A. V., Biesecker, D. A., Kohl, J. L., 2002, *ApJ*, 571, 1008
- Suess, S. T., Nerney, S. F., 2002, *ApJ*, 565, 1275
- Tappin, S. J., Simnett, G. M., Lyons, M. A., 1999, *A&A*, 350, 302
- Tu, C.-Y., Marsch, E., 1995, *Space Sci. Rev.*, 73, 1
- Tu, C.-Y., Marsch, E., 1997, *Solar Phys.*, 171, 363
- Tu, C.-Y., Marsch, E., 2001, *JGR*, 106, 8233
- Tu, C.-Y., Marsch, E., Wilhelm, K., Curdt, W., 1998, *ApJ*, 503, 475
- Uzzo, M., Ko, Y.-K., Raymond, J. C., 2004, *ApJ*, 603, 760
- Vásquez, A. M., Raymond, J. C., 2004, *ApJ*, submitted
- Vocks, C., Marsch, E., 2002, *ApJ*, 568, 1030
- Voitenko, Y., Goossens, M., 2003, *Space Sci. Rev.*, 107, 387
- Voitenko, Y., Goossens, M., 2004, *ApJ*, 605, L149
- Wang, Y.-M., 1994, *ApJ*, 435, L153
- Wang, Y.-M., Sheeley, N. R., Jr., Socker, D. G., Howard, R. A., Rich, N. B., 2000, *JGR*, 105, 25133
- Wentzel, D. G., 1989, *ApJ*, 336, 1073
- Whang, Y. C., 1997, *ApJ*, 485, 389
- Wiegmann, T., Schindler, K., Neukirch, T., 2000, *Solar Phys.*, 191, 391
- Zangrilli, L., Nicolosi, P., Poletto, G., Noci, G., Romoli, M., Kohl, J. L., 1999, *A&A*, 342, 592